JOURNAL OF THERMOPHYSICS AND HEAT TRANSFER
Vol. 8, No. 4, Oct.–Dec. 1994

Direct Simulation of Diatomic Gases Using the Generalized Hard Sphere Model

D. B. Hash*
North Carolina State University, Raleigh, North Carolina 27695
James N. Moss†
NASA Langley Research Center, Hampton, Virginia 23681
and
H. A. Hassan‡
North Carolina State University, Raleigh, North Carolina 27695

The generalized hard sphere model that incorporates the effects of attraction and repulsion is examined. First, the model is used to study simple adiabatic heat baths. Then, it is used to predict flow measurements in tests involving extremely low freestream temperatures. For the two cases considered, a Mach 26 nitrogen shock and a Mach 20 nitrogen flow over a flat plate, only rotational excitation is deemed important, and appropriate modifications for the Borgnakke-Larsen procedure are developed. In general, for the cases considered, the present model showed a modest improvement over the variable hard sphere model.

Nomenclature

c_r	=	relative velocity
E_c	=	total collision energy
E_i	=	collision internal energy
E_r	=	rotational energy
E_t	=	relative translational energy
f	=	distribution function
k	=	Boltzmann constant
m_r	=	reduced mass
n	=	number density
P	=	inelastic collision probability
T	=	temperature
T^0	=	reduced temperature
T_r	=	rotational temperature
$\bar{t}$	=	average number of collisions per particle
R_f	=	random fraction
r	=	intermolecular distance
Z	=	relaxation number
$\alpha_1, \alpha_2, \omega_1, \omega_2$	=	generalized hard sphere parameters
Γ	=	gamma function
ε	=	potential well-depth energy
ε_i	=	particle internal energy
ζ	=	internal DOF
η	=	inverse power law exponent
κ, κ'	=	force constants
ν, ν'	=	attractive-repulsive force law exponents
σ	=	intermolecular separation at which potential is zero
σ_T	=	total collision cross section
τ_c	=	mean collision time
Ω	=	collision integral
ω	=	variable hard sphere exponent

Received Oct. 8, 1993; revision received Feb. 17, 1994; accepted for publication Feb. 17, 1994.

*Research Assistant, Mechanical and Aerospace Engineering. Student Member AIAA.

†Research Engineer, Aerothermodynamics Branch, Space Systems Division. Fellow AIAA.

‡Professor, Mechanical and Aerospace Engineering. Associate Fellow AIAA.

Introduction

THE direct simulation Monte Carlo (DSMC) method of Bird[1] has been very successful at accurately simulating low-density flows. To implement the method, a collision model must be selected. The most widely used model is the variable hard sphere (VHS) model of Bird.[2] In this model, molecules scatter like hard spheres, and the total cross section has a velocity dependence typical of a repulsive inverse power law. The exponent of the power law is inferred from viscosity measurements. For flow conditions where the temperature ranges from tens to thousands of degrees, one exponent is not sufficient to fit the viscosity data. The generalized hard sphere (GHS) model[3,4] overcomes this problem by employing an interaction model that allows for both attraction and repulsion.

Most of the low-density experimental tests are carried out in facilities where the freestream temperature is of the order of tens of degrees Kelvin. At such temperatures, the attractive part of an interaction potential cannot be neglected. In order to be able to interpret test results accurately, a DSMC formulation with an interaction potential that allows for both attraction and repulsion must be used. The GHS model provides such a potential. Therefore, the goal of this work is to investigate the usefulness of the GHS model in predicting flow properties in existing test facilities. Two cases are selected for this investigation: 1) a Mach 26 nitrogen shock[5] and 2) a Mach 20 nitrogen flow over a flat plate.[6] In both of these experiments, rotational excitation plays an important role. Because of this, expressions needed for the implementation of the Borgnakke-Larsen[7] procedure for rotational relaxation were developed for the GHS model. In addition, it became evident that the widely used rotational relaxation number developed by Parker[8] is only valid for a hard sphere model. The expression was rederived for both the VHS and GHS models; however, in order to insure comparisons only between the collision models, the same rotational relaxation numbers were employed in all simulations. Results using both collision models were compared with the shock measurements of Smith.[5]

GHS Model

The generalized hard sphere model can be thought of as a simple extension of the VHS model that allows for both attraction and repulsion. In both models, molecules scatter like

hard spheres. The total cross section for the VHS model can be written as

$$\frac{\sigma_T}{\sigma_{T,\text{ref}}} = (c_r^2/c_{r,\text{ref}}^2)^{-\omega} = (E_t/E_{t,\text{ref}})^{-\omega}$$
$$E_t = \tfrac{1}{2}m_r c_r^2 \tag{1}$$

while the GHS model assumes

$$(\sigma_T/\sigma^2) = \sum \alpha_j (E_t/\varepsilon)^{-\omega_j} \tag{2}$$

The ω in Eq. (1) is related to the exponent of the repulsive force

$$F = (\kappa/r^\eta) \quad \text{by} \quad \omega = [2/(\eta - 1)] \tag{3}$$

On the other hand, if two terms in the series indicated in Eq. (2) are considered, then ω_1 and ω_2 are related to the exponents of a repulsive, weakly attractive force of the type

$$F = (\kappa/r^\nu) - (\kappa'/r^{\nu'}) \tag{4}$$

by

$$\omega_1 = \frac{2}{\nu - 1}, \qquad \omega_2 = \frac{2 + \nu - \nu'}{\nu - 1} \tag{5}$$

The parameters α_1 and α_2 are determined from viscosity or binary diffusion data or their related cross sections, depending on whether the interaction is between like or unlike molecules. The parameters ω_1 and ω_2 can be inferred in the same way or, by choosing a particular interaction law, i.e., Lennard-Jones (12-6) potential for which $\omega_1 = \frac{1}{6}$ and $\omega_2 = \frac{2}{3}$.

This GHS model can be incorporated into all the expressions necessary for the DSMC method such as the probabilities for collision, internal energy exchange, and reactions. The expressions for these quantities are given in Ref. 4.

Low Enthalpy Nitrogen Flows

The flows considered in this work[5,6] exhibit low-temperature regions in which the attractive portion of the potential is important. These type of flows are examined to demonstrate the advantages of using the GHS model compared to the traditional VHS model. All the considered flows consist of a single diatomic gas: nitrogen. The flows have a low total enthalpy such that no reactions or vibrational excitation occurs.

The only interaction that must be modeled is that of the N_2-N_2 collision. Because of the need for low-temperature accuracy, the viscosity cross sections of Neufeld et al.[9] have been used to determine the parameters in the GHS expression. These empirical equations allow the calculation of the viscosity collision integral, $\Omega^{(2,2)}$, for the Lennard-Jones (12-6) potential for reduced temperatures in the range $0.3 \leq T^0 \leq 100$ with error less than 0.03% ($T^0 = kT/\varepsilon$). The parameters σ and ε/k for nitrogen are taken from Svehla[10] and are 3.798 Å and 71.4 K, respectively. Table 1 gives the parameters for the GHS model for this interaction, and Fig. 1 gives a comparison of the first approximation to the viscosity between the correlation, the GHS, and VHS models. The parameters for the VHS model for nitrogen were taken from Bird[2] and are given in Table 2.

Table 1 Parameters for GHS model for nitrogen for temperatures up to 2500 K

α_1	α_2	ω_1	ω_2
2.32842	6.54333	0.0280087	0.777166

Table 2 Parameters for VHS model for nitrogen

ω	d_{ref}, Å
0.24	4.07

From Fig. 1, it is seen that the GHS model reproduces the viscosity at lower temperatures more accurately than the VHS model. In fact, the GHS model accurately reproduces the viscosity over the entire temperature range shown. This leads to an important point about the GHS model; it can be used for any temperature range and is not just specific to low-temperature applications.

The main difference between the two models can be seen through their representation of the quantity $\sigma_T c_r/(\sigma_T c_r)_{\max}$. This quantity represents the collision probability for a pair of molecules selected at random in a given cell. Figure 2 compares $\sigma_T c_r$ for a repulsive, attractive, and attractive-repulsive potential. As seen from the figure, the quantity increases with an increasing relative velocity for a repulsive potential, and decreases with an increasing relative velocity for an attractive potential. In other words, the majority of collisions for repulsive potentials involve particles with the higher energies, whereas the majority of collisions for attractive potentials involve particles with the lower energies. The situation is a hybrid of the two for attractive-repulsive potentials. For higher temperatures or higher average relative velocities, repulsive collisions will dominate. For much lower temperatures or lower average relative velocities, attractive collisions will dominate. The figure demonstrates that without the attractive component the VHS model has no way of accounting for the tendency of attractive collisions to dominate at lower temperatures.

Since the flows considered involve internal energy, a mechanism for internal energy exchange must be employed. For

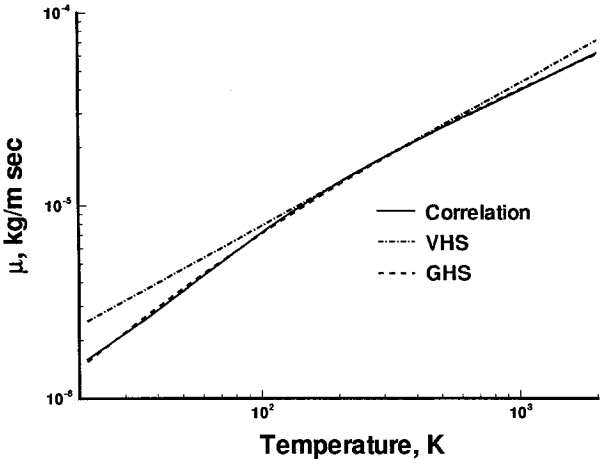

Fig. 1 Viscosity coefficient for nitrogen.

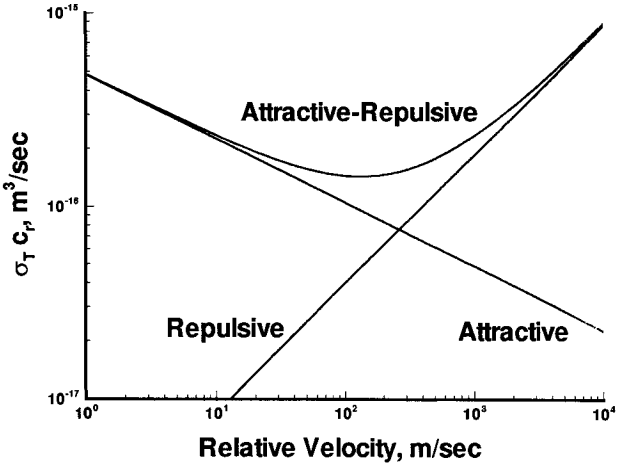

Fig. 2 Behavior of collision probabilities for different potentials.

the DSMC method, this is traditionally done with the Borgnakke-Larsen[7] method. This method has been modified for the GHS model, and those modifications along with all the necessary expressions for implementation of the method follow.

Borgnakke-Larsen Model

The Borgnakke-Larsen model for polyatomic gases is outlined next. In this model, a fraction of the collisions are regarded as completely inelastic, and new values of the internal and translational energies are sampled from equilibrium distributions. The remainder of the collisions are regarded as elastic, and no internal energy exchange occurs. The following section describes the partitioning of energy when a collision is determined to be inelastic.

The internal energy of a collision pair is the sum of the internal energies of the components

$$E_i = \varepsilon_{i,1} + \varepsilon_{i,2} \tag{6}$$

The distribution function for the internal energy of a single molecule can be written as[11]

$$f_{\varepsilon_{i,1}} \propto \varepsilon_{i,1}^{(\zeta_1/2)-1} \exp(\varepsilon_{i,1}/kT) \tag{7}$$

where ζ_1 is the number of internal DOF of molecule 1, i.e.

$$\zeta_1 = \zeta_{r,1} + \zeta_{v,1}$$

where subscripts r and v refer to rotation and vibration. The total fraction of pairs with internal energy E_i is proportional to f_{E_i} where[1]

$$f_{E_i} \propto E_i^{\zeta-1} \exp(-E_i/kT) \tag{8}$$

where $\zeta = [(\zeta_1 + \zeta_2)/2]$. It is shown in Ref. 4 that the distribution of E_t is given by

$$f_{E_t} = \frac{2}{m_r^2}\left(\frac{m_r}{kT}\right)^{3/2} \sqrt{(2/\pi)}\, \frac{\sigma_T}{\sigma_T c_r} E_t \exp(-E_t/kT) \tag{9}$$

The total energy E_c in the collision is the relative translational energy and the combined internal energy, i.e.

$$E_c = E_t + E_i$$

The probability of a particular pair of values E_t and E_i is proportional to the product of f_{E_i} and f_{E_t}, or

$$f_{E_t} f_{E_i} \propto \sigma_T E_t (E_c - E_t)^{\zeta-1} \exp(-E_c/kT) \tag{10}$$

For each inelastic collision, a postcollision value E_t^* is sampled from this distribution by the acceptance-rejection method. This entails finding the maximum of Eq. (10) and taking the ratio of Eq. (10) to its maximum. Let

$$x = (E_t/\varepsilon), \qquad \xi = (E_c/\varepsilon)$$

then the maximum of Eq. (10) follows from determining the maximum of the quantity

$$G(x) = (\alpha_1 x^{1-\omega_1} + \alpha_2 x^{1-\omega_2})(\xi - x)^{\zeta-1}$$

Setting the derivative of $G(x)$ to zero gives

$$(\xi - x)^{\zeta-2}[\alpha_1(\omega_1 - \zeta)x^{1-\omega_1} + \alpha_2(\omega_2 - \zeta)x^{1-\omega_2} + \alpha_1\xi(1-\omega_1)x^{-\omega_1} + \alpha_2\xi(1-\omega_2)x^{-\omega_2}] = 0 \tag{11}$$

Ignoring $x = \xi$, the root x^* is found by iteration. The normalized distribution function is obtained from

$$F(x) = G(x)/G(x^*) \tag{12}$$

When $\zeta = 1$, x^* is chosen as ξ. This same choice is made with the VHS model. The acceptance-rejection method is implemented as follows. The current random number R_f (between 0–1) gives

$$E_t = R_f E_c, \qquad E_i = E_c - E_t \tag{13}$$

Eq. (13) is substituted into Eq. (12), and the value of F is compared with another R_f. If $F < R_f$, another choice of R_f is made and the process is repeated. Otherwise, Eq. (13) is accepted. The internal energy is divided in a manner similar to that employed in Ref. 1.

The additional iteration required to find the maximum of Eq. (10) is a major disadvantage of the GHS model because it decreases computational efficiency. The Borgnakke-Larsen method provides an average split of energies equal to the ratio of the DOF of the mode being partitioned to the total number of DOF to ensure detailed balance. Because of this, we can replace f_{E_t} in Eq. (9) by a Hinshelwood type distribution [see Eq. (7)] with a ζ_t given from

$$\bar{E}_t = (\zeta_t/2)kT \tag{14}$$

where

$$\zeta_t = 2\left\{2 - \omega_1 + \frac{\omega_1 - \omega_2}{(\alpha_1/\alpha_2)[\Gamma(2-\omega_1)/\Gamma(2-\omega_2)](kT/\varepsilon)^{\omega_2-\omega_1} + 1}\right\} \tag{15}$$

With this choice, all computational procedures employed in the VHS computation can be implemented for the GHS model. The only additional complexity is that resulting from a calculation of a cell temperature. This approximation will allow for detail balance; i.e., all modes, if allowed to relax to equilibrium, will converge to the same temperature. The simplification in the numerical procedure outlined above yields the correct macroscopic properties. However, the details of the distribution will be different because Eq. (9) is not exactly of the type indicated in Eq. (7).

A crucial part of the Borgnakke-Larsen method is the determination of the probability of an inelastic collision. For many years, it was thought that this probability should be written as

$$P = (1/Z) \tag{16}$$

However, this is not true in general; the form of the probability function largely depends on the selection methodology used in employing the probability and the relaxation rate equation specified. The details of the proof cannot be presented here due to its length, but have been thoroughly explicated in Haas et al.[12]

The present work uses a pair selection methodology for the Borgnakke-Larsen method in which the probability is applied to the pair of colliding particles, and both relax if the event is accepted. This is in contrast to the typical selection methodology used in Bird's codes: the particle selection method in which each colliding particle is checked for relaxation. From considerations of Jeans[13] equation as related to the Borgnakke-Larsen model, Lumpkin et al.[14] have shown that the correct choice of the probability for the pair selection methodology for rotational relaxation is

$$P_R = [(1 + \zeta_R/\zeta_t)/Z_R] \tag{17}$$

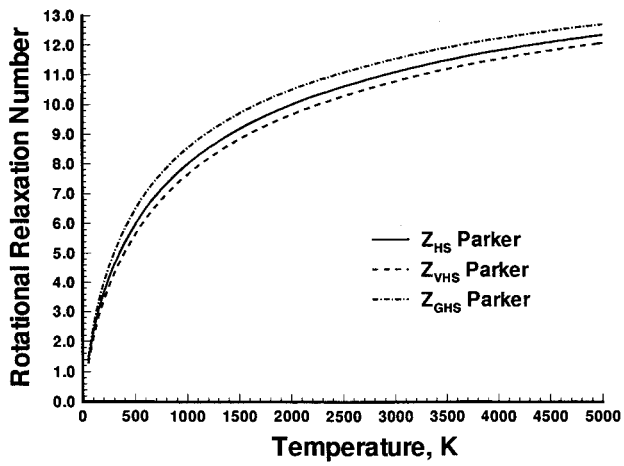

Fig. 3 Theoretical and experimental rotational relaxation numbers for nitrogen.

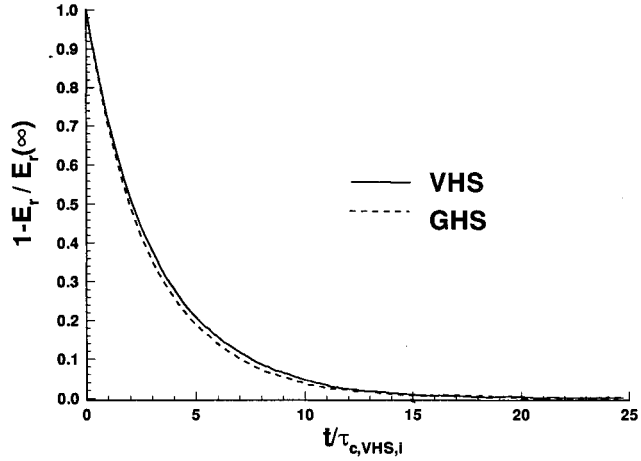

Fig. 4 Adiabatic heat bath relaxation with T_t = 1000 K.

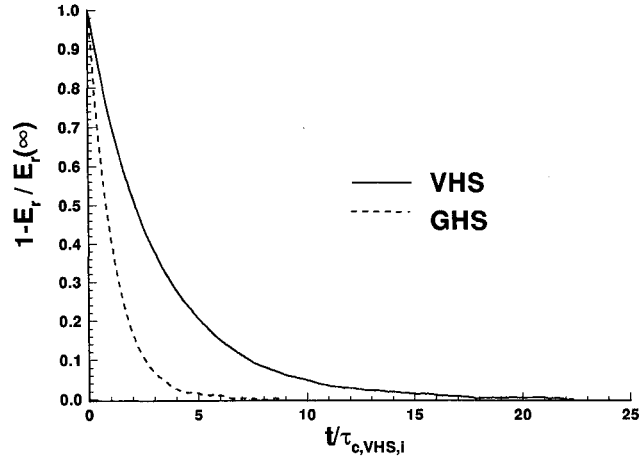

Fig. 5 Adiabatic heat bath relaxation with T_t = 20 K.

where ζ_t is the relative translational DOF, ζ_R is the sum of the rotational DOF of the colliding molecules, and Z_R is the rotational relaxation number. An expression similar to Eq. (17) for the particle selection method is derived in Ref. 12. Results using this model produce the same results as the pair selection model as long as the correct probabilities are used in each case. As such, they are included here.

Recent investigators using a temperature-dependent relaxation number for Z_R have employed Parker's formula [Eq. (45) of Ref. 8]. This widely used formula is obtained by integrating Eq. (40) in Ref. 8, assuming a hard sphere model. Thus, the formula must be adjusted if an interaction model other than a hard sphere model is used. Making the same approximation introduced by Parker in order to obtain an analytical expression for Z_R, one finds that for a variable hard sphere model, the formula takes the form

$$Z_R = \frac{\frac{\Gamma(3-\omega)}{2} Z_{R,\infty}}{\frac{\Gamma(3-\omega)}{2} + \frac{2\pi}{3}\Gamma\left(\frac{5}{2}-\omega\right)\left(\frac{T^*}{T}\right)^{1/2} + \left(\frac{\pi^2}{4}+2\right)\Gamma(2-\omega)\left(\frac{T^*}{T}\right)} \tag{18}$$

For the GHS model, Parker's formula is

$$Z_R = \frac{\left[\sum \alpha_j \left(\frac{T^*}{T}\right)^{\omega_j} \Gamma(2-\omega_j)\right] \frac{2-\omega_1}{2} Z_{R,\infty}}{\sum \alpha_j \left(\frac{T^*}{T}\right)^{\omega_j} \left[\frac{\Gamma(3-\omega_j)}{2} + \frac{2\pi}{3}\Gamma\left(\frac{5}{2}-\omega_j\right)\left(\frac{T^*}{T}\right)^{1/2} + \left(\frac{\pi^2}{4}+2\right)\Gamma(2-\omega_j)\left(\frac{T^*}{T}\right)\right]} \tag{19}$$

Both expressions reduce for a hard sphere model to the original Parker formula corrected by Brau and Jonkman.[15] Figure 3 shows the comparisons between the different Parker formulas for typical constants used for nitrogen.

GHS Model Validation

In order to make sure that the GHS model has been implemented correctly, several simulations of the thermal relaxation of the translational and rotational modes of nitrogen in an adiabatic heat bath have been carried out. For these test cases, all energy is assumed initially to be in the translational mode with the rotational mode being vacant. The energies are then allowed to relax toward equilibrium. A constant rotational relaxation number of 5 is specified for all simulations. Two separate conditions are considered: 1) a high-temperature case with an initial translational temperature of 1000 K and 2) a low-temperature case with an initial translational temperature of 20 K. For both conditions, the VHS and GHS models are employed. Figure 4 depicts the rotational relaxation plotted in time for both models for the high-temperature case. The time axis is normalized by the initial mean collision time for the VHS model denoted by $\tau_{c,VHS,i}$. In the figure, E_r is the rotational energy, and $E_r(\infty)$ is the equilibrium value of the rotational energy. Both models predict similar relaxation at this high temperature because the effect of the attractive component in the GHS model is negligible. Figure 5 depicts a drastically different result for the low-temperature case. The relaxation as determined with the GHS model is significantly faster than that calculated by the VHS model. Here, we see clearly the importance of the attractive term in the GHS model. To be sure that all results were calculated correctly, the relaxation of the rotational energy was plotted vs the average number of collisions per particle denoted as $\tilde{\tau}$ (Fig. 6). As discussed in Haas et al.,[12] all

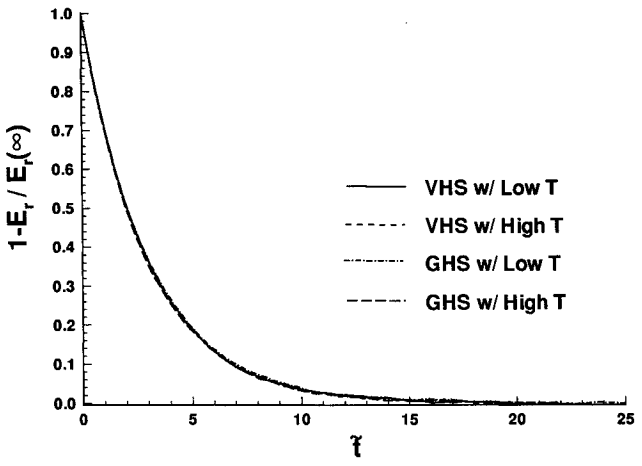

Fig. 6 Adiabatic heat bath results plotted against the average number of collisions per particle.

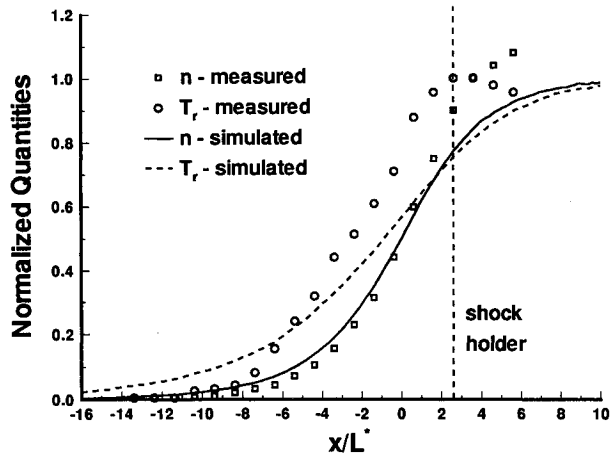

Fig. 7 Uncorrected VHS simulation of Mach 26 nitrogen shock wave.

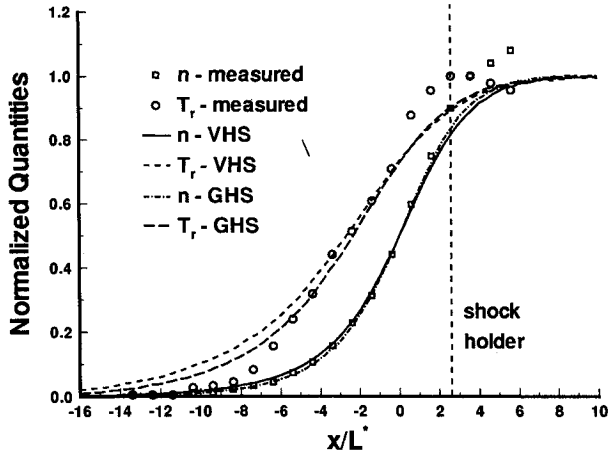

Fig. 8 VHS and GHS simulations of Mach 26 nitrogen shock wave.

the curves should coincide. This is the case that validates the implementation of the GHS model.

Results

One-Dimensional Nitrogen Shock Calculations

The GHS model is used to simulate the Mach 26 nitrogen shock wave experiment by Smith.[5] In this experiment, nitrogen is expanded in a conical nozzle in which a cylindrical brass shock holder is positioned. The electron-beam fluorescence technique is employed, and measurements of density and rotational temperature through the shock were obtained. The stagnation temperature and pressure for the experiment were 1300 K and 200 psia, respectively, corresponding to low-enthalpy conditions. Thus, reactions and vibrational excitation could be neglected in the simulation. The full experimental flow is not simulated; instead, a one-dimensional normal shock is used to represent the experiment. In order to measure the usefulness of the GHS model, comparisons are made between it, the VHS model, and the experiment.

Recently, Boyd[16] has also considered this experiment using the VHS model and a Sutherland viscosity model. It should be noted that the Sutherland viscosity model is a special case of the GHS model with $\omega_1 = 0.0$ and $\omega_2 = 1.0$. In his investigation, Boyd used a limiting value of Z_R of 18 with a value of T^* of 91.5 K as suggested by Mason and Monchick.[17] These parameters have been adopted for this investigation.

To stress the importance of using the appropriate relaxation probabilities, Fig. 7 shows the results obtained using the VHS model without the correction suggested by Lumpkin et al.[14] using Parker's original formula. The modified Parker's formulas were not used, because this would result in the imposition of different relaxation numbers for the two cases. It was important for the comparisons to be made only between the collision rates of the models so as to determine the effect of attraction. As is seen from the figure, the comparison to the measurements of rotational temperature is extremely poor. Also, the overall shock thickness is overpredicted.

Figure 8 provides the results for both the GHS and VHS models using Parker's original formula using the corrected probabilities. As reported by Smith,[5] the data in the rear portion of the shock is not reliable due to heat transfer effects between the gas and the brass shock holder. Given this, comparison for both the GHS and VHS models is good in the forward portion of the shock. The GHS shows an improvement over the VHS model in producing a thinner shock. Because of the extremely cold temperature upstream, the attractive portion of the potential is important. The GHS collision frequency is increased over that of the VHS model in the cold temperature region due to the modeling of the effects of attraction, thus providing a more accurate simulation of the shock thickness. The predictions of the number density distributions are excellent; however, neither model is predicting the rotational temperature well in the most forward portion of the shock. One possible explanation is that the experiment of Smith may have had some trace impurity that would have caused faster relaxation rates. Another could be errors associated with measuring the rotational distribution at low temperatures.[5] These issues are just some of the factors that complicate efforts to simulate rotational relaxation. Nonetheless, the GHS model shows improvement over the VHS model for the value of $Z_{R,\infty}$ employed.

Flat Plate Heat Transfer Calculations

Recently, at the Eighteenth International Symposium on Rarefied Gas Dynamics, Allègre et al.[6] presented experimental measurements of density and surface heat flux for a flat plate with a truncated leading edge in a hypersonic low-density nitrogen flow. The experiment was conducted in a wind tunnel in which the flow expanded through a conical nozzle. The experimentalists report the existence of both transverse and longitudinal gradients through the test section. Thus, the flow around the flat plate is decidedly three dimensional. However, for the sake of simplicity, the investigators assumed the flow to be two dimensional in the plane of symmetry, and carried out both two-dimensional Navier-Stokes and DSMC calculations to compare with their experiments. One particular case was of significant interest. For this case, the upstream Mach number was 20 with a Reynolds number of 8.38×10^3 based on the flat plate length of 10 cm. The stagnation temperature and pressure were 1100 K and 10 bars, respectively, corresponding to low-enthalpy condi-

tions. For this particular case, the investigators acquired a very good comparison between the Navier-Stokes and experimental measurements of surface heat flux. However, the DSMC results showed as much as a 50% difference between the simulation and experiment. Since the experimental error in the heat transfer measurements was reported not to have exceeded 10%, it would appear that the DSMC method is not capturing some important aspect of the physics of the problem.

It is the purpose of this investigation to explore the reasons in the discrepancy between the DSMC and experimental results. The upstream temperature for this experiment was 14 K. Since the attractive portion of the potential well is important at such a cold temperature, it is thought that more accurate modeling of the interaction law using the GHS model may lead to improved results. A second explanation for the discrepancy might be the fact the upstream conditions were nonuniform because of the use of a conical nozzle as described by Allègre et al.[18]

The present investigators also assumed the flow over the plane of symmetry of the flat plate to be essentially two dimensional. As seen in Fig. 9, the grid used for this simulation depicts a two-dimensional flat plate with a blunt leading edge of finite thickness, and is composed of 6 regions and 6300 cells. Both GHS and VHS models were employed with and without freestream nonuniformities, and all calculations used an accommodation coefficient of 1. Also, calculations were carried out using an infinitely thin flat plate simulation of the experiment using the VHS model employing 4275 cells. Figure 10 shows the experimental heat transfer distribution compared with the calculations of Allègre et al. and the present investigators. There is a discrepancy between the infinitely thin flat plate results and the finite thickness results over the first tenth of the plate. Besides this, all DSMC calculations compare very well to one another, and none compare well to the experiment. The effect of introducing the GHS model or the freestream nonuniformities had little effect on the heat transfer calculations as well as the density calculations. Figure

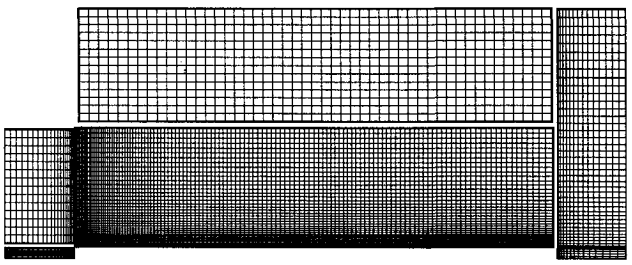

Fig. 9 Grid for flat plate simulation.

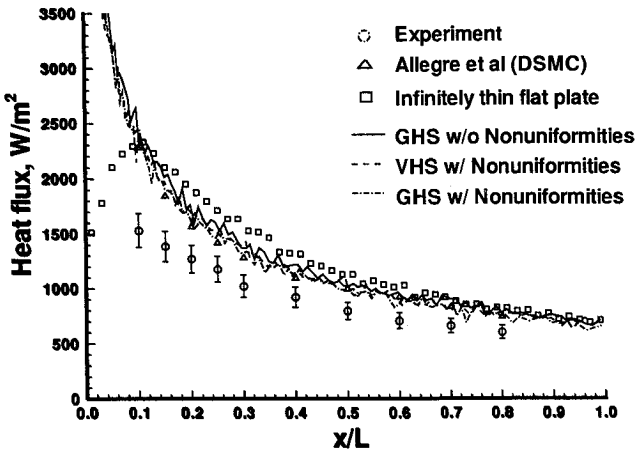

Fig. 10 Flat plate heat transfer distributions.

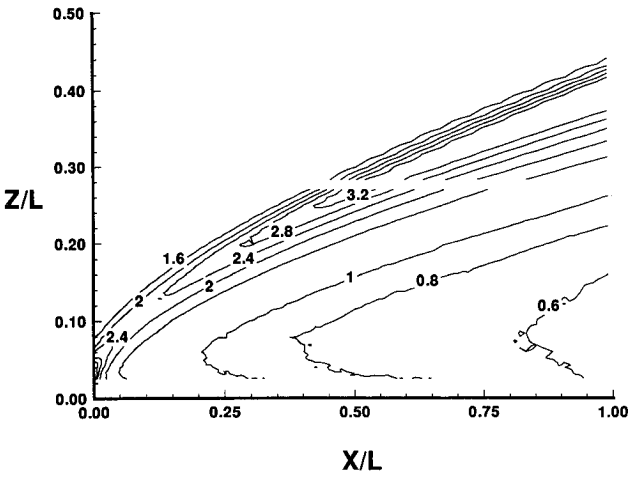

Fig. 11 Flowfield density contours for the GHS simulation with freestream nonuniformities.

11 shows the density contours normalized with respect to freestream for the GHS model with freestream nonuniformities. The results obtained here compare reasonably well to the results given by Allègre and Raffin[19] for the lower portion of the shock. However, the discrepancy between the DSMC and experimental results for the surface heat transfer is still left to be explained. It is possible that because of the conical nature of the nozzle a three-dimensional simulation of the entire nozzle and test section might be necessary in order to accurately capture the physics of this problem. Recently, Nance[20] has simulated this experiment using the three-dimensional DSMC code of Rault et al.[21] He was unable to reproduce the experimental data. Instead, his results show agreement with the other DSMC simulations that would discount the effects of the three-dimensional nature of the flow in the plane of symmetry. It is possible, but unlikely, that a better means of modeling the gas-surface interaction is necessary. All DSMC simulations discussed to this point have used accommodation coefficients of 1; a slightly lower accommodation factor would decrease the heat transfer calculations. Allègre et al.[6] did see a slight improvement in their results for similar flat plate experiments using an accommodation coefficient of 0.8. However, because we are dealing with an engineering surface, it is expected that full accomodation is achieved. Finally, simulations assumed that the experimentally quoted Mach and Reynolds numbers were correct. If this was not the case, then a possible explanation for the discrepancies between experiment and simulation may result.

Concluding Remarks

Based on simple heat bath calculations, differences are noted between the GHS and VHS models at low temperatures. Because the GHS model gives a better fit of the viscosity over a much wider temperature range, it is deemed that it is an improvement over the VHS model. Small differences between the two models were noted in the two experiments investigated. This suggests that the mean flow properties compared are not very sensitive to the collision models employed.

Acknowledgments

This work is supported in part by a National Science Foundation Graduate Fellowship, NASA's Cooperative Agreement NCCI-112, and the Mars Mission Research Center funded by NASA Grant NAGW-1331. The authors would like to acknowledge many helpful discussions with Brian Haas of the NASA Ames Research Center, and Ken Sutton and Roop Gupta of the NASA Langley Research Center.

References

[1]Bird, G. A., *Molecular Gas Dynamics*, Clarendon Press, Oxford, England, UK, 1976.

[2]Bird, G. A., "Monte Carlo Simulation in an Engineering Context," *Rarefied Gas Dynamics*, edited by S. S. Fisher, Vol. 74, Pt. I, Progress in Astronautics and Aeronautics, AIAA, New York, 1981, pp. 239–255.

[3]Hash, D. B., and Hassan, H. A., "Monte Carlo Simulation Using Attractive-Repulsive Potentials," Eighteenth International Symposium on Rarefied Gas Dynamics, 1992.

[4]Hassan, H. A., and Hash, D. B., "A Generalized Hard Sphere Model for Monte Carlo Simulation," *Physics of Fluids A*, Vol. 5, No. 3, 1993, pp. 738–744.

[5]Smith, R. B., "Electron-Beam Investigation of a Hypersonic Shock Wave in Nitrogen," *Physics of Fluids*, Vol. 15, No. 6, 1972, pp. 1010–1017.

[6]Allègre, J., Raffin, M., Chpoun, A., and Gottesdiener, L., "Rarefied Hypersonic Flow over a Flat Plate with Truncated Leading Edge," Eighteenth International Symposium on Rarefied Gas Dynamics.

[7]Borgnakke, C., and Larsen, P. S., "Statistical Collision Model for Monte Carlo Simulation of Polyatomic Gas Mixtures," *Journal of Computational Physics*, Vol. 18, No. 4, 1975, pp. 405–420.

[8]Parker, J. G., "Rotational and Vibrational Relaxation in Diatomic Gases," *Physics of Fluids*, Vol. 2, No. 4, 1959, pp. 449–462.

[9]Neufeld, P. D., Janzen, A. R., and Aziz, R. A., "Empirical Equations to Calculate 16 of the Transport Collision Integrals $\Omega^{(l,s)*}$ for the Lennard-Jones (12-6) Potential," *Journal of Chemical Physics*, Vol. 57, No. 3, 1972, pp. 1100–1102.

[10]Svehla, R. A., "Estimated Viscosities and Thermal Conductivities of Gases at High Temperatures," NASA TR R-132, 1962.

[11]Hinshelwood, C. N., *The Kinetics of Chemical Change*, Oxford Univ. Press, Oxford, England, UK, 1940.

[12]Haas, B. L., Hash, D. B., Bird, G. A., Lumpkin, F. E., and Hassan, H. A., "Rates of Thermal Relaxation in Direct Simulation Monte Carlo Methods," *Physics of Fluids* (to be published).

[13]Jeans, J. H., *The Dynamical Theory of Gases*, Cambridge Univ. Press, London, 1916.

[14]Lumpkin, F. E., Haas, B. L., and Boyd, I. D., "Resolution of Differences Between Collision Number Definitions in Particle and Continuum Simulations," *Physics of Fluids A*, Vol. 3, No. 9, 1991, pp. 2282–2284.

[15]Brau, C. A., and Jonkman, R. M., "Classical Theory of Rotational Relaxation in Diatomic Gases," *Journal of Chemical Physics*, Vol. 52, No. 2, 1970, pp. 477–484.

[16]Boyd, I. D., "Temperature Dependence of Rotational Relaxation in Shock Waves of Nitrogen," *Journal of Fluid Mechanics*, Vol. 246, Jan. 1993, pp. 343–360.

[17]Mason, E. A., and Monchick, L., "Heat Conductivity of Polyatomic and Polar Gases," *Journal of Chemical Physics*, Vol. 36, No. 6, 1962, pp. 1622–1639.

[18]Allègre, J., Dubreuilh, X. H., and Raffin, M., "Aerodynamic Forces Applied to a Delta Wing Located in Rarefied Hypersonic Flows," *Workshop on Hypersonic Flows for Reentry Problems: Part II*, Antibes, France, April 1991.

[19]Allègre, J., and Raffin, M., "Champs D'ecoulements Hypersoniques au Voisinage D'une Plaque Plane," Rapport SESSIA 331/89.866, Aug. 1989.

[20]Nance, R. P., private communication, North Carolina State Univ., Raleigh, NC, Aug. 1993.

[21]Rault, D. F. G., Wilmoth, R. G., and Bird, G. A., "An Efficient DSMC Algorithm Applied to a Delta Wing," AIAA Paper 91-1316, June 1991.